

# Nano Sensor Networks for Tailored Operation of Highly Efficient Gas-To-Liquid Fuels Catalysts

Eisa Zarepour<sup>1</sup>      Mahbub Hassan<sup>1</sup>      Chun Tung Chou<sup>1</sup>  
Adesoji A. Adesina<sup>2</sup>

<sup>1</sup> School of Computer Science and Engineering  
University of New South Wales, Australia  
{ezarepour, mahbub, ctchou} @cse.unsw.edu.au

<sup>2</sup> ATODATECH LLC, Brentwood, CA 94513 USA  
ceo@atodatech.com

**Technical Report**  
**UNSW-CSE-TR-201318**  
**July 2013**

THE UNIVERSITY OF  
NEW SOUTH WALES



School of Computer Science and Engineering  
The University of New South Wales  
Sydney 2052, Australia

## Abstract

Fischer-Tropsch synthesis, a major process for converting natural gas to liquid hydrocarbons (GTL) suffers from selectivity limitations. While GTL reactor produces highly useful hydrocarbons in the form of liquid fuels such as gasoline, it also produces low-grade hydrocarbons such as methane. Selectivity refers to the ratio of highly useful hydrocarbons to the total product output. The literature is replete with various catalyst formulations which seek to improve selectivity to specific product spectrum via for example, molecular size or shape exclusion using zeolites or control of growing surface chain length with particle (site) geometry. Existing strategies for selectivity improvement, such as manipulation of reactor operating factors (temperature, pressure, etc) and catalyst design preparation variables may be classified as top-down approaches.

In this work, a bottom-up approach is proposed in which surface processes can be controlled via Nano Sensor Network (NSN) involving the turning on or off of elementary steps consisting undesired species, and redirection of surface efforts to step(s) leading to the wanted products. The overall effect of this nano-level communications will lead to superior selectivity than hitherto possible by reducing the rate of Hydrogenation To Paraffin (HTP) reactions.

Our numerical and simulation results reveal an exponential relationship between reduction in rates of HTP reactions and selectivity. It also confirms a considerable improvement of overall selectivity in a catalyst that is equipped by a high reliable NSN in comparison with extant catalyst technologies and current commercial Fischer-Tropsch reactors <sup>1</sup>.

---

<sup>1</sup> This work was done while the last author was with the School of Chemical Engineering at University of New South Wales.

# 1 Introduction

Gas-to-liquid (GTL) compounds are clean fuels and intermediates for the production of other petrochemicals. Fischer-Tropsch (FT) synthesis is the main process for converting natural gas to the liquid hydrocarbons [1]. However, the reaction is a complex network of many other steps and the requirement for efficient use of the reactants ( $H_2$  and CO) to yield specified product spectrum (e.g. only olefins of a particular narrow product weight distribution) is critical and measured in terms of selectivity - a reaction index termed.

$$Selectivity = \frac{d}{T} \quad (1.1)$$

which  $d$  is amount (or rate of formation) of the desired products and  $T$  is amount (or rate of formation) of both desired and unwanted products. The conversion of synthesis gas to clean fuels and olefins suffers from selectivity limitations because the reaction is a polymerization scheme in which surface unsaturated hydrocarbons are the precursors to olefins and paraffins via desorption and hydrogenation. There are many factors that affect the selectivity of FT. Process conditions, such as temperature, pressure and reactant ratio, as well as catalyst composition influence the selectivity [2, 3]. Improving selectivity of FT selectivity by controlling these factors is an ongoing area of intense research activities [2, 3, 4, 5, 6, 7, 8, 9].

In this work, we propose a new approach to improve selectivity via using Nano Sensor Networks (NSNs) which are formed by establishing communication between devices made from nano-materials. The objective of the present work is to propose a NSN, a network of nano-machines, which can be used to turn off pathways leading to unwanted products e.g. termination to paraffin and/or amplify the desorption of olefinic surface species. Unlike the conventional control of  $H_2$ :CO ratio in the reactor feed, the Nano-machine will have to work at atomic or molecular level to exert control in the middle of chemical reactions (after certain steps are completed). This bottom-up approach is evident in many biological processes and responsible for the high selectivity and specificity accompanying these reactions (e.g. ATP hydrolysis, photosynthesis, etc).

The contributions of this paper can be summarised as follows:

- We propose a novel methodology to improve chemical synthesis output by using NSNs and specifically examine the idea for FT reactor to improve product selectivity.
- We propose an analytical model for FT reactor based on discrete time Markov Chain (MC) and calculate selectivity and product distribution of FT via this model.
- We also design and run a simulation based on Stochastic Simulation Algorithm (SSA) and the results confirm analytical model output.
- Based on numerical and simulation results, NSN can improve product selectivity and this boosting has an exponential relationship with reduction in the rate of hydrogenation to paraffin (HTP) reactions.

The rest of this paper is structured as follows. Section II provides some general information about the NSNs. Section III reviews the FT synthesis specifications. In Section IV we discuss the idea of using NSNs to improve selectivity.

Section V provides an analytical model based on Markov chain to evaluate the idea followed by SSA simulation framework in Section VI. Some key challenges discuss in Section VII and conclusions are given in section VIII.

## 2 Nano sensor networks

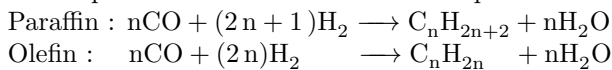
Technically, a NSN is a network of nano-scale devices capable of some basic computing, sensing, actuation, and communication tasks. The seminal paper by Akyildiz et al. [10] shows that conceptually it is possible to achieve communication at nano-scale either using electromagnetic or some form of molecular-based transceivers. This has sparked a flurry of new research activities in a bid to understand the unique properties of nano-materials that could be utilized for communication between nano devices [11, 12, 13, 14, 15].

Because a NSN can work at atomic levels, they can be used for totally new kind of nanotechnology applications which cannot be realized with conventional sensor networks. Akyildiz and Jornet [11] has outlined a number of interesting new applications of NSNs in biomedical, environmental, industrial, and military domains. In all these applications, distributed communication between nano-machines are envisaged to accomplish the application goal.

In this paper, our goal is to explore the potential of NSN in improving product selectivity of FT synthesis. A NSN deployed on the catalyst surface would be able to monitor all the reactions and intermediate steps. This makes it possible to intervene the FT process and divert the product path from paraffin to olefin in a more direct and efficient way.

## 3 Fischer- Tropsch

Fischer-Tropsch synthesis, a major process for converting natural GTL hydrocarbons is a complex process involving many intermediate chemical reactions or steps, but we can depict the overall function using the black-box of figure 3.1. Two top level reactions of FT can be expressed as:



There are two inputs,  $\text{H}_2$  and  $\text{CO}$  which are fed to a FT reactor in a predetermined ratio.

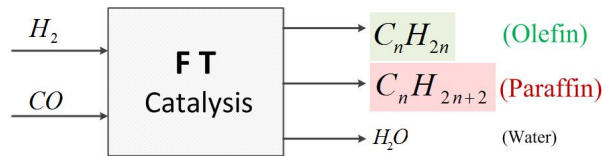


Figure 3.1: Input and output of Fischer-Tropsch Catalysis.

After several intermediate reactions which have been shown in table 3.1 [3], we obtain two main products, viz; olefin ( $\text{C}_n\text{H}_{2n}$ ) and paraffin ( $\text{C}_n\text{H}_{2n+2}$ ). Olefins are unsaturated hydrocarbons used as building blocks for making other

petrochemicals and polymers in a wide variety of industrial and consumer markets such as packaging, transportation, electronic, textile, and construction [16, 17, 18].

In contrast, paraffins are saturated hydrocarbons that cannot be used for further product development and therefore have low commercial value. Thus, the olefin-paraffin ratio is an important reactor performance index.

### 3.1 Intermediate Steps and Elementary Reactions

It is important to understand the elementary reactions in the FT chemistry if we want to control at molecular-level, which is precisely the objective of NSN. Table I shows the elementary reactions involved in the conversion of  $H_2$  and CO to olefins and paraffins [3].

<b>Adsorption phase</b>	
	$CO + s \rightleftharpoons CO_s$
	$CO_s + s \rightleftharpoons C_s + O_s$
	$H_2 + 2s \rightleftharpoons 2 H_s$
<b>Surface reactions</b>	
<b>Water formation</b>	$O_s + H_s \rightleftharpoons HO_s + s$
	$HO_s + H_s \rightleftharpoons H_2O + 2s$
<b>Chain initiation</b>	$C_s + H_s \rightleftharpoons CH_s + s$
	$CH_s + H_s \rightleftharpoons CH_{2s} + s$
	$CH_{2s} + H_s \rightleftharpoons CH_{3s} + s$
<b>Chain growth</b>	$C_n H_{2n+1s} + CH_{2s} \rightleftharpoons C_{m+1} H_{2m+3s} + s$ ( $m=n+1$ ), $r = k_p$
<b>Hydrogenation to Paraffin (HTP)</b>	$C_n H_{2n+1s} + H_s \rightleftharpoons C_n H_{2n+2} + 2s$ $r = k_{tp}$
<b><math>\beta</math>-Dehydrogenation to Olefin (BTO)</b>	$C_n H_{2n+1s} \rightleftharpoons C_n H_{2n} + H_s$ $r = k_{to}$

Table 3.1: Hydrocarbon synthesis via Fischer-Tropsch [3]

All reactions take place on the surface of a catalyst. Before a reaction can take place, reactants must first be adsorbed onto the catalytic surface. The surface of a catalyst contains sites where reactants can be adsorbed. A CO may dissociate into C and O atoms. Similarly,  $H_2$  also adsorb to produce two hydrogen atoms. A  $CH_2$  is formed when a C reacts with two neighboring H molecules and a  $CH_2$  in turn may react with an adjacent H to form a  $CH_3$ . A  $CH_3$  can either react with a H to form a  $CH_4$  (methane) or it may kick start a chain growth by reacting with an adjacent  $CH_2$ , forming intermediate species

$C_nH_{2n+1}$ , which are the precursors to both olefins and paraffins. A  $C_nH_{2n+1}$  can either lead to olefin, i.e.,  $C_nH_{2n}$ , through desorption or dehydrogenation (losing one H), or paraffin, i.e.,  $C_nH_{2n+2}$ , through hydrogenation (adding one H). In order to improve the FT selectivity, our NSN aims to reduce the occurrence of the latter reaction.

### 3.2 Current effort to improve FT selectivity

Many attempts have been made to promote selectivity of FT and they can be categorized as two main groups of controlling operational factors (temperature, pressure, etc) and catalyst design preparation variables. In the first category, researchers try to improve selectivity by manipulating the environmental factors of reactor such as pressure, temperature and CO:  $H_2$  feeding ratio [2, 3].

Thermodynamics considerations alone often show that conditions favorable for the production of the desired product are also good (if not better) for forming the unwanted materials. This is why we have waste products in many chemical processes including even some important biological reactions. Therefore, we cannot rely on thermodynamics alone to help us improve selectivity.

In the surface of the catalyst, several efforts are trying to develop novel catalyst such as nanostructured catalyst to improve selectivity [6, 7, 19, 20, 21, 22, 23, 24]. However, in a system, where an inorganic catalyst is used to speed up the reaction rate, rrxn, it is often the case that both the rate of wanted and undesired products are accelerated in accordance with the law,

$$r_{rxn} = f_1(C)e^{\left(\frac{-E_{rxn}}{R_gT}\right)} \quad (3.1)$$

where  $f_1(C)$  is a function expressing the dependency of rate on concentration of reactants and products while  $E_{rxn}$  is the activation energy for the reacting species on the particular catalyst. The conventional wisdom in catalysis is to design a suitable catalyst where  $E_{rxn}$  for the desired product is considerably lower than for any other product(s) or indeed the entire reaction.

In this work, we introduce a completely novel approach that would give the control of the surface of the catalyst to increase the rate of wanted products via decreasing the Hydrogenation to Paraffin (HTP) reactions rates by NSNs. Indeed each site of the surface of the catalyst would be equipped by a nano machine to control operations in that site and also is able to communicate with its neighbors sites. For this reason, a clear understanding from the surface of the catalyst is necessary.

### 3.3 Surface of FT catalyst

The surface of a catalyst contains numerous sites or special locations where reactants can be adsorbed and react with each other. Many studies have been carried out to model the structure of the active sites in the surface of the catalyst [25, 20, 26]. Before modeling the surface we need some evidences from the surface of real catalysts to find out the morphology of sites. It can be achieved through techniques such as high-resolution scanning tunneling microscopy (STM) [25], X-ray absorption spectroscopy (XANES, X-ray absorption

near-edge spectroscopy) [20], scanning electron microscopy (SEM) and transmission electron microscopy (TEM) [20] to investigate and elucidate the atomic-scale structure of the catalytic surfaces. For instance, STM provides a direct, real-space investigation and structural specification of matter at the atomic level based on quantum tunneling. It also can provide essential insight about active sites and any defects in the surface of the catalyst. Figure 3.2 shows two different STM pictures from the surface of a catalyst with nickel surface.

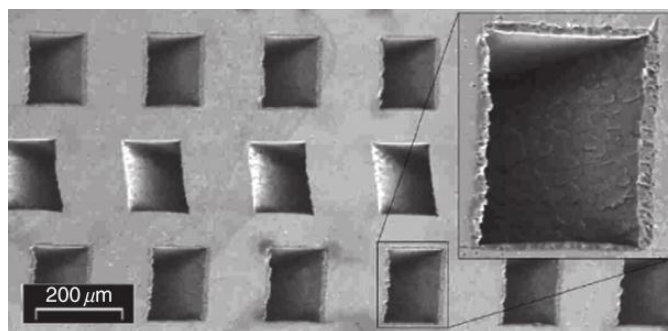


Figure 3.2: Two STM images of the nickel (1 1 1) surface with 2% (right) and 7% (left) gold coverage, respectively [20].

In recent years, there has been significant progress in the production of nano-structured catalysts which means the surface of the catalyst can be fashioned in a predefined morphology at the micro- or nano-scale [19, 27, 23]. In [19] different types of micro-structured catalytic reactors have also been investigated. Figure 3.3 shows a catalyst with a 2D grid morphology that has been developed via a thin porous layer of alumina on a metal surface [19].

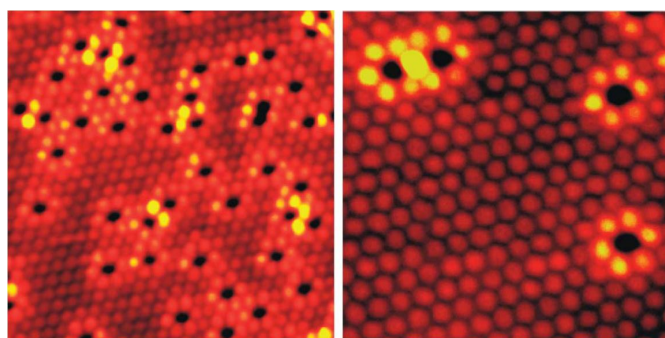


Figure 3.3: A scanning electron microscopy (SEM) image from the surface of a micro-structured catalyst [19].

Based on this real pictures from the surface of the catalyst, the morphology

of the surface can be considered as a regular grid. For instance, in [26] a grid with a dimension of 66\*66 sites has been used to simulate FT synthesis via a KMC simulation tools. Also the authors have assumed all reactions take place on three-fold hollow sites that has depicted in figure 3.4.

As a result, the surface of the catalyst can be assumed as a fixed total number of reactive sites in a 2D grid structure but in reality the site locations may follow other structures. However, the precise site distribution is not a concern at this time. Each one of these sites can be either vacant or occupied by only one atom or molecule. The number of atoms or molecules adsorbing on sites is proportional to the concentration in the gas phase, or equivalently to the partial pressure  $P$ , and to the number of vacant sites.

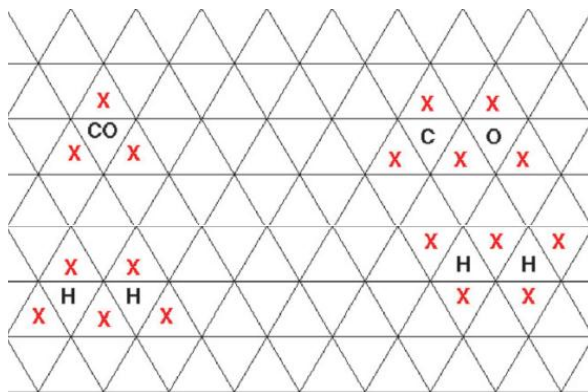


Figure 3.4: A schematic which has been used to model surface of the catalyst [26]. Triangles are sites and reactant must adsorb into these sites before any reaction take place.

## 4 Selectivity control with NSNs

In this part, we propose a novel approach in which surface processes may be controlled via nano-machines involving the turning on or off of elementary steps (at periodic/aperiodic intervals) involving undesired species, and redirection of surface efforts to step(s) leading to the wanted products. First we will provide a general architecture for NSN and then explain how it can control selectivity.

### 4.1 Proposed Architecture

Recent advancements in electronic enabled nano-materials such as carbon nanotubes and graphene have paved the way for the new generation of electronic nano-components like nano-sensor, nano-memories, nano-batteries and even nano-processors [11].

Although nano-devices are not yet available commercially, there are significant relevant developments in recent years that point to a future when such



termed hydrogenation to paraffin (HTP). Therefore, the aim of NSN would be to prevent H from reacting with  $C_nH_{2n+1}$  as much as possible.

Assuming that a H and  $C_nH_{2n+1}$  would react only if these two species come close to each other, say reside in neighboring sites of a catalyst surface, then one way to reduce reaction rate of HTP would be to control the location of H adsorption on the catalyst surface based on the knowledge of current content of each site.

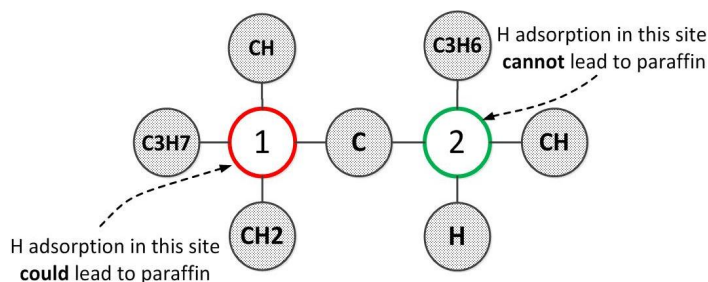


Figure 4.2: An example snapshot from the surface of a catalyst. There are two unoccupied sites, each having four neighbours occupied with different molecule species. Hydrogen adsorption in site 1 can lead to a paraffin because of the presence of an  $C_3H_7$  in the neighbourhood, but its adsorption in site 2 cannot produce any paraffin.

For example, figure 4.2 shows the content of a number of sites (represented by circles) on the catalyst surface. There are two unoccupied sites, marked as 1 and 2. If an H is adsorbed at site 1, then it could lead to paraffin due to presence of  $C_nH_{2n+1}$  ( $C_3H_7$ ) in the neighborhood, but an adsorption of an H at site 2 cannot lead to the production of paraffin. Therefore, the NSN should allow H adsorption for site 2, but prevent it for site 1.

Such spatial control of H adsorption on a catalyst surface could be achieved with an NSN in the following ways. More specifically, each nano-sensor is capable of sensing two events: (1) a  $C_nH_{2n+1}$  has just formed at the site from an elementary reaction and (2) an H is attempting to adsorb to the currently unoccupied site. In detection of first event, the nano-machine should update a local binary variable, which indicates whether the site currently contains a  $C_nH_{2n+1}$ . In detection of the second event, nano-machine queries all the neighboring nano-machines via its transmitter to learn whether there exists a  $C_nH_{2n+1}$  in the neighborhood (neighborhood search). If  $C_nH_{2n+1}$  is present in the neighborhood, the nano-machines should prevent the H adsorption via its actuator (say by reflecting it back to the feed gas which would be a basic actuation task), but allow the adsorption otherwise.

It means a nano-machine can process and decide whether the current adsorbed molecule which is in site should be desorbed or not. This decision making will be based on information which obtain from neighbors and can be implemented by pre-programming each nano-machine with the following algorithm to be executed in a loop forever via its nano-processor:

---

Hydrogen Sensing and Control Algorithm for all nanomachine

---

```

for ever do
  if Site_Content == CnH2n+1s and receives a search query then
    | Transmit an acknowledgment to the sender
  if an H is attempting to occupy site and CnH2n+1s is present in the
    | neighbourhood then Prevent H adsorption

```

---

Figure 4.3: Hydrogen Sensing and Control Algorithm for all nanomachine

The outcome of the above algorithm is following. If a site forms HS within another site in its neighborhood containing (C<sub>n</sub>H<sub>2n+1s</sub>), it will immediately deactivate the HS to reduce the probability of forming paraffin (note: paraffin is formed when (C<sub>n</sub>H<sub>2n+1s</sub>) binds with HS). The overall impact of the NSN is reduction in the rate of HTP reactions. Note that the proposed nano-machine meets its target without requiring any of the nano-sensors moving physically.

As NSNs are in the early stage of development and deployment of a real NSN on the surface of the catalyst is not possible yet, an analytical model and extensive simulations have been done to evaluate proposed framework. In next part, we describe an analytical framework to model Fischer-Tropsch synthesis and also investigate the effects of any reduction in HTP reaction rates on the selectivity and product distribution.

## 5 Modelling using Markov Chain

A network of chemical reactions can be modelled by a Continuous Time Markov Chain whose states are all different possible chemical compositions during the reaction [31]. A Continuous Time Markov Chain can be approximated by a Discrete Time Markov Chain (MC) with a sufficiently small sampling time interval [32].

In such MC model, any consuming or producing of input, intermediate or output species or any changing in their populations leads to changing in the state of the system. For example, a simple reaction such as  $A + B \rightarrow C$  with initial composition of  $A=1, B=1$  and  $C=0$  can be considered as a MC with two different states of  $S_0$  ( $A=1, B=1, C=0$ ) and  $S_1$  ( $A=0, B=0, C=1$ ). In this simple instance, if we increase initial reactants then number of states will increase. For instance, if we put  $A=2, B=2$  it leads to 3 different states of  $S_0$  ( $A=2, B=2, C=0$ ),  $S_1$  ( $A=1, B=1, C=1$ ),  $S_2$  ( $A=0, B=0, C=2$ ).

The probability of transition from one state to another state can be obtained from reaction rate  $r$ , ( $r = X_A * X_B * k$ ; that  $X_A/X_B$  is number of molecules of species A/B respectively in that specific state and  $k$  is kinetic constant of the reaction). For instance in a system with two possible reactions of  $R_1$  and  $R_2$  to move from  $S_1$  to  $S_2$  with rate of  $r_1=66$  and  $r_2=33$ , the probability of transition from  $S_1$  to  $S_2$  via  $R_1$  is  $66/99$  (0.66) and via  $R_2$  is  $33/99$  (0.33).

A. Problem Formulation In our application, FT reactor, system starts with

specified molecules of CO and  $H_2$  and states changes as far as there is a possibility to take place any intermediate reaction based on Table I. In each state, all possible reactions, based on current composition, would be considered to generate complete state space. System stops in some states when there is no further possible reaction called absorbing states in MC terminology and that means once system entered in these states, will never leave. By definition, state  $i$  is absorbing when  $P(i,i) = 1$  and hence  $P(i,j) = 0$  for all  $j \neq i$ . Absorbing state is not unique and in some scenarios system can terminate in many different absorbing states with different probabilities. Probability of eventually reaching to each of these absorbing states can be extracted from fundamental matrix that obtains by performing some operation on the transition probability matrix [33].

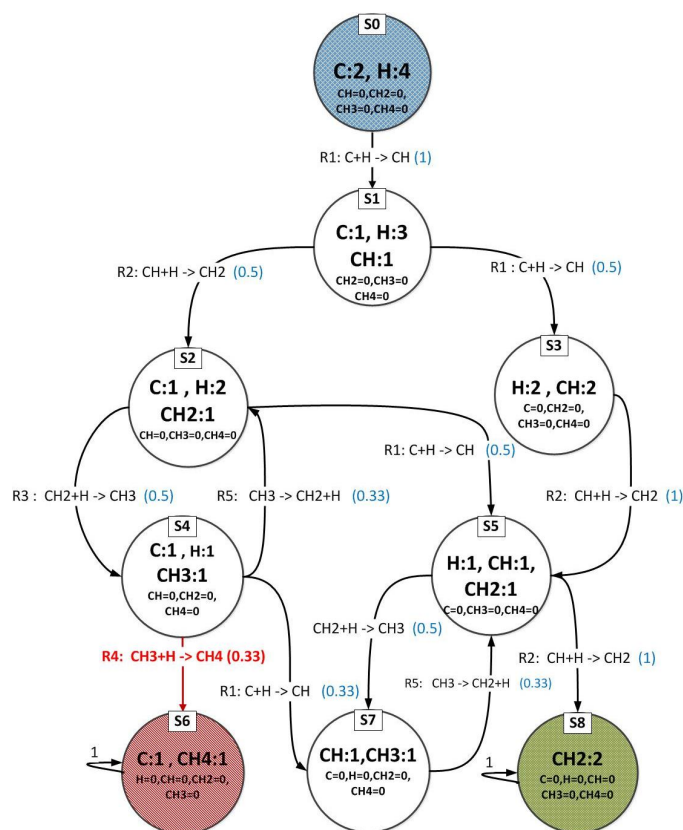


Figure 5.1: A modelling of a simple FT synthesis via a Markov chain for an initial reactants of C=2, H=4.  $S_6$  and  $S_8$  are absorbing states. The blue number in the parentheses are probability of transition from one state to another state. NSN goal is reducing the rate of HTP reactions e.g. in this sample it would try to reduce probability of going from state 4 to state 6 via  $R_4$ .

Figure 5.1 demonstrates a snapshot of a very small MC model from the surface of the FT synthesis with only 2 and 4 starting species of Carbon and Hydrogen respectively. For simplification of this instance, we ignore water for-

mation reactions but in the analytical model and also simulation we consider the whole intermediate reactions of FT. In this example, due to small number of initial molecules, we have only five reactions that have been mentioned in Table II. System starts from initial states ( $S_0$ ) with 2 molecules of carbon and 4 molecules of hydrogen. The only possible reaction based on composition of  $S_0$  is  $R_1$  ( $C + H \rightarrow CH$ ) that leads to transit to state 1 with probability of 1 via  $R_1$ . Then system can move via two different paths; to  $S_3$  via  $R_1$  ( $C + H \rightarrow CH$ ) or  $S_2$  via  $R_2$  ( $CH + H \rightarrow CH_2$ ). As the rate of  $R_1$  and  $R_2$  based on composition of state 2 are equal then these two transitions have equal probabilities of 0.5. The rest of probable states and possible transitions have been depicted in the figure 5.1.

R <sub>1</sub>	Chain initiation	$C_s + H_s \rightleftharpoons CH_s + s$
R <sub>2</sub>		$CH_s + H_s \rightleftharpoons CH_{2s} + s$
R <sub>3</sub>		$CH_{2s} + H_s \rightleftharpoons CH_{3s} + s$
R <sub>4</sub>	Hydrogenation to Paraffin (HTP)	$CH_{3s} + H_s \rightleftharpoons \mathbf{CH_4} + 2s$
R <sub>5</sub>	$\beta$ -Dehydrogenation to Olefin (BTO)	$CH_{3s} \rightleftharpoons \mathbf{CH_2} + H_s$

Table 5.1: REACTIONS OF FIGURE 5.1.

There are 9 different compositions in this sample and state  $S_6$  and  $S_8$  are absorbing states and also final states that means there is no further possible reactions based on composition of these two states. As NSN aims to reduce HTP reactions rates, we focus on  $S_4$  that is a potential state for HTP reactions.  $S_4$  has three different options; back to the  $S_2$  with 33%, move to  $S_7$  with 33% or transit to  $S_6$  with probability of 0.33 via a HTP reaction ( $CH_3 + H \rightarrow CH_4$ ). In order to capture the effect of NSN in the MC model we assume NSN would be able to reduce rate of all HTP reactions by  $\delta$  percentage. For example, in case of  $\delta=20$  that means NSN can reduce rate of HTP reactions by 20%, in figure 5.1 the probability of going from state 4 to state 6 via R6 will decrease by 20% and drops from 0.33 to around 0.266.

## 5.1 Calculating selectivity via analytical model

As we model FT system as a MC, composition of absorbing states can be considered as final probable composition to calculate selectivity and product distribution analysis. We consider all olefins and paraffins species in all possible absorbing states to extract overall selectivity. For example, in sample of figure 5.1 selectivity of  $S_6$  is 0 because there is no olefin in its composition. At the other hand, as there are two  $CH_2$  in  $S_8$  without any paraffin, selectivity of  $S_8$  is 1. In a real F-T, system eventually converge to one of these absorbing states. Hence, it is necessary to involve probability of reaching these absorbing states to calculate selectivity and analyse product distribution.

Probability of eventually reaching a specific absorbing state m from initial state 0 can be extracted from fundamental matrix [33] of our MC model. If we have n states and a transition probability matrix of P (n-by-n) then fundamental

matrix can be obtained as:

- Re-number the states so that the absorbing states are the first  $f$  states. As a result, the one-step transition probability matrix will take the form of  $P$

$$P = \begin{pmatrix} I & 0 \\ R & Q \end{pmatrix}$$

which  $I$  is  $f$ -by- $f$  identity matrix,  $0$  is a  $f$ -by- $(n-f)$  zero matrix,  $R$  is a rectangular sub-matrix giving transition probabilities from non-absorbing to absorbing states,  $Q$  is the square sub-matrix giving these probabilities from non-absorbing to non-absorbing states.

- Calculate fundamental matrix  $N$  as :

$$P^2 = \begin{bmatrix} I & 0 \\ R & Q \end{bmatrix} \begin{bmatrix} I & 0 \\ R & Q \end{bmatrix} = \begin{bmatrix} I & 0 \\ R+QR & Q^2 \end{bmatrix},$$

$$P^3 = \begin{bmatrix} I & 0 \\ R+QR & Q^2 \end{bmatrix} \begin{bmatrix} I & 0 \\ R & Q \end{bmatrix} = \begin{bmatrix} I & 0 \\ R+QR+Q^2R & Q^3 \end{bmatrix},$$

$$P^t = \begin{bmatrix} I & 0 \\ (I+Q+Q^2+\dots+Q^{t-1})R & Q^t \end{bmatrix}.$$

$$P^\infty = \begin{bmatrix} I & 0 \\ NR & 0 \end{bmatrix} \quad N = I + Q + Q^2 + \dots = (I - Q)^{-1}$$

In this case matrix of  $B=NR$  gives the probability of eventually reaching to absorbing states.  $B(i,j)$  is the probability of eventually reaching to absorbing state  $j$  from non-absorbing state  $i$ . For instance, in sample of figure 5.1 after performing all those steps  $B(0,6) = 0.102$ ,  $B(0,8) = 0.898$ .

Generally, to analyze the output of each experiment based on MC model, we process the composition of each absorbing state  $S_j$  to extract amount of olefin ( $C_nH_{2n}$ ) as  $Ole_j$  and paraffin ( $C_nH_{2n+2}$ ) as  $Par_j$ . Then we calculate total olefins/paraffins as:

$$Olefin = \sum_{j=1}^m Ole_j * B(0, j) \quad ; \quad Paraffin = \sum_{j=1}^m Par_j * B(0, j)$$

Which  $B(0,j)$  is probability of reaching absorbing state  $j$  from initial state and  $m$  is number of absorbing states in the model. After extracting total olefins/paraffins we use Equation (1.1) to calculate overall selectivity.

## 5.2 Numerical Experiments

We examine the idea based on this model for initial molecules of  $CO_5$  and  $H_{15}$ . It implies  $n \leq 5$  meaning that the chain growth is limited to  $C_5H_{11}$ , i.e., the

longest olefin and paraffin produced would be, respectively,  $C_5H_{10}$  and  $C_5H_{12}$ . Thus, based on Table I we have a total of 20 reactions (3 chain initiation, 5 chain growth, 2 water formation, 5 hydrogenation to paraffin and 5 dehydrogenation to olefin). Similarly, we have a total of 21 species including C, H, CH, O, OH,  $H_2O$ , 5 intermediate species as  $(C_nH_{2n+1})$ , 5 final olefin products  $(C_nH_{2n})$ , and 5 final paraffin products  $(C_nH_{2n+2})$ . We assume kinetic constant of all 20 different reactions is 7. With this setting, after running the model in MATLAB, we found system has 3271 different states (different distinct possible compositions) with 257 different absorbing states.

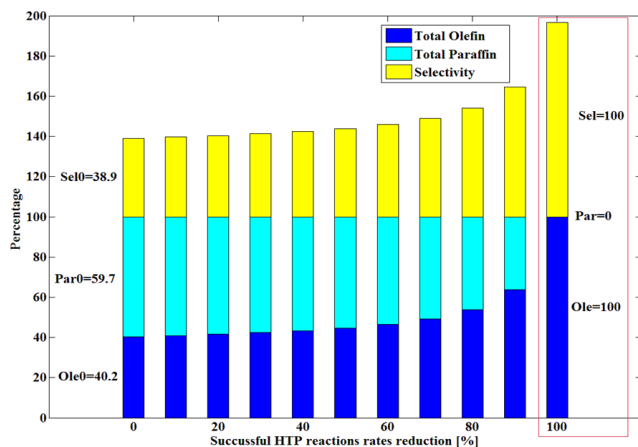


Figure 5.2: Product distribution and selectivity after running the analytical model with initial molecules of CO: 5 and H: 15 for 10 different scenarios of HTP rate reduction ( $\delta$  from 0 to 100%).

Figure 5.2 shows changing in product distribution and selectivity for any value of  $\delta$ , reduction in HTP reaction rates. The direct implication of reduction in HTP rates is increasing the ratio of olefin and also decreasing in amount of paraffin species. Olefin ratio starts from 40.2% when there is no reduction in HTP and reaches 100% when the NSN would be able to cut off all HTP reaction. Paraffin drops from 59.7% to 0 and selectivity raises from 38.9% to 100%. shows changing in product distribution and selectivity for any value of  $\delta$ , reduction in HTP reaction rates.

In figure 5.3 there is a clear trend of increasing in selectivity with more successful reduction in HTP reactions rates. Selectivity starts from around 40% in a normal synthesis without any changing in reactions rates ( $\delta=0$ ) and reaches to 100% in case of no HTP reaction ( $\delta=1$ ). We found there is an exponential relationship between  $\delta$  and selectivity.

Figure 5.4 reveals partial selectivity of different hydrocarbons in the model. It shows hydrocarbons with higher degree have less selectivity in any assumed value of  $\delta$  and that points to a natural phenomenon in a real FT reactor.

For large and complex systems, traditional Markov models face with the state explosion problem and quickly become intractable [34]. In this experiment as

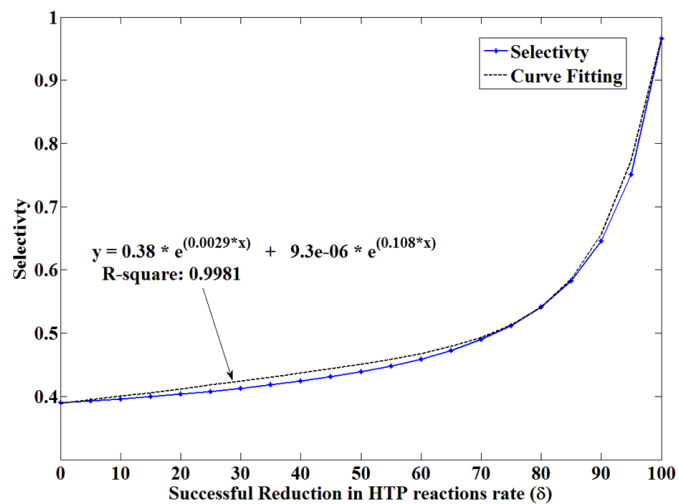


Figure 5.3: Selectivity for different successful reduction in HTP reaction rates based on results of model with initial molecules of CO: 5 and H: 15.

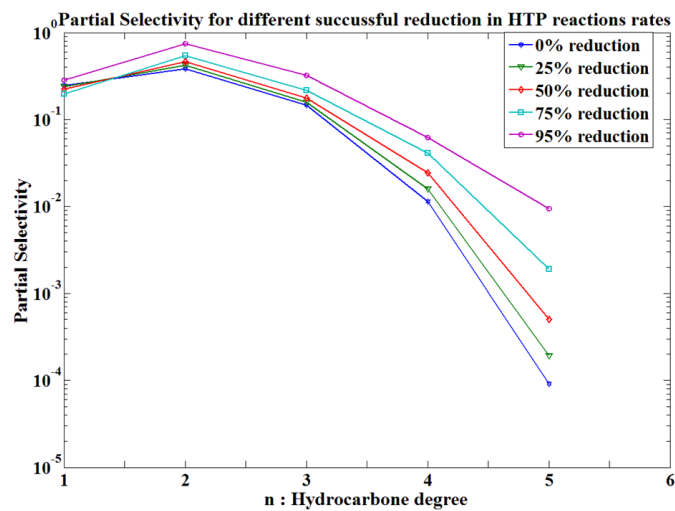


Figure 5.4: Partial selectivity of hydrocarbon with degree smaller than 6 in 5 different successful reductions in HTP reduction rates.

we have different types of intermediate reactions and also MC model considers all possible reactions in all possible states, it generates a huge state space. For example, in case of only 10 initial molecules of CO and 20 molecules of H we have more than 35000 different states which is huge in terms of required computational power and memory to build and solve the model. To run such simple instance for 21 different amount of  $\delta$ , ranging from 0 to 100% we used a cluster of 21 machines with 84 cores and totally 168GB ram for 35 hours. Figure 5.5 Shows how state space exponentially grows with linear increasing of the feeding molecules.

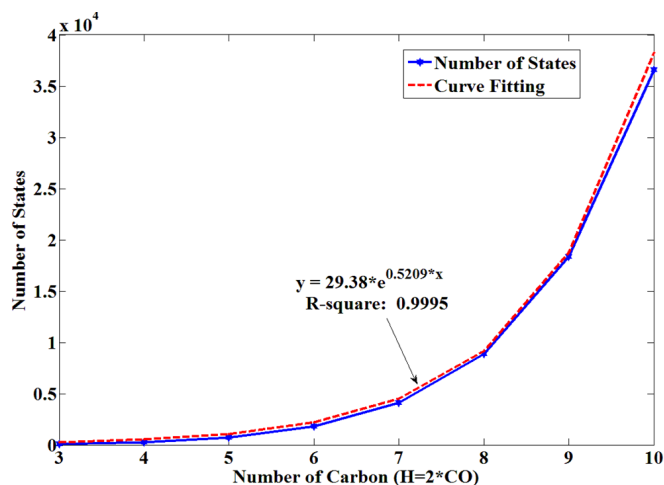


Figure 5.5: State Space complexity. Number of states in MC model grows exponentially with increasing number of initial molecules. For a scenario with just CO=10 and H=20 molecules we have 36593 different states.

Due to such limitations, a real FT synthesis cannot be modeled via a MC framework. However, we can use a standard simulation algorithm (SSA) that benefits from Markov model and also produces a smaller state space by choosing one of possible reactions in each states. In next section, simulation via SSA would be presented.

## 6 Simulation

Chemical reactions can be modeled by Markov chains and a standard algorithm to simulate them is the Stochastic Simulation Algorithm (SSA) by Gillespie [35]. The standard SSA algorithm takes three inputs: (1) a set of reactions, (2) a set of kinetic constants corresponding to each reaction, and (3) initial counts for each species, which define the initial state of the simulation. In general, the state in SSA is defined as the number of each chemical species in the system. At each state, the simulator determines a candidate reaction to take place from the set of all possible reactions and updates the state (species counts) accordingly.

Simulation stops when there are no reactions to take place. The output of the algorithm is the number of each chemical species at the end of the simulation.

## 6.1 SSA Platform

We consider a FT catalysis with  $n \leq 10$ . It means, we have a total of 36 species including C, H, CH, O, OH, H<sub>2</sub>O, 10 intermediate species as (C<sub>n</sub>H<sub>2n+1</sub>), 10 final olefin products (C<sub>n</sub>H<sub>2n</sub>), and 10 final paraffin products (C<sub>n</sub>H<sub>2n+2</sub>). We set the initial species counts as C=10000, H=20000, and zero for all other species. Figure 6.1 shows how the states change for a given simulation. We can see that although we start with only two species, C and H, new species start to form as different reactions take place during the simulation. At the end of the simulation, we analyze all olefin and paraffin products and the resulting selectivity for the simulated FT catalysis.

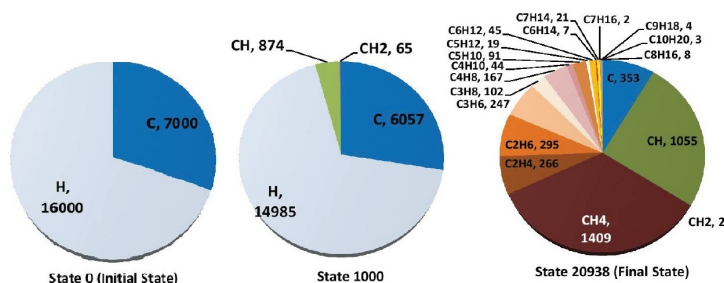


Figure 6.1: A snapshot of state changes during simulation (CO=7000,H=16000). Species concentrations continue to evolve as elementary reactions take place.

Although there are a total of 34 kinetic constants for 34 reactions in 4 different categories (based on Table I), for simplification, it can be assumed that all reactions in a given category have the same kinetic constant. We simulated a total of 4 different sets of kinetic constants. We only present results for the set where all  $k = 7$ , as the results for other settings were similar.

To simulate the effect of proposed NSNs in the surface of the catalyst we assume a successful reduction in HTP reactions of  $\delta$  and then we run an experiment with a modified  $k_{tp}$  (kinetic constant of HTP group of reactions) that has been decreased by  $\delta$ . Other kinetic constants remain same. For each of the 4 sets of kinetic constants, we simulated a total of 21 different  $\delta$  ranging from 0 to 100%, leading to a total of  $4 \times 21 = 84$  simulation configurations. For each configuration, the simulation is repeated 10 times and the average results over 10 runs are presented.

## 6.2 Simulation Results

In order to validate the numerical and simulation results first we compare selectivity over  $\delta$  for both numerical and simulation for initial setting of CO=5 and H=15.

We found the simulation results are similar to the results of Markovian model which has been depicted in figure 6.2. Hence, we just mention two main graphs

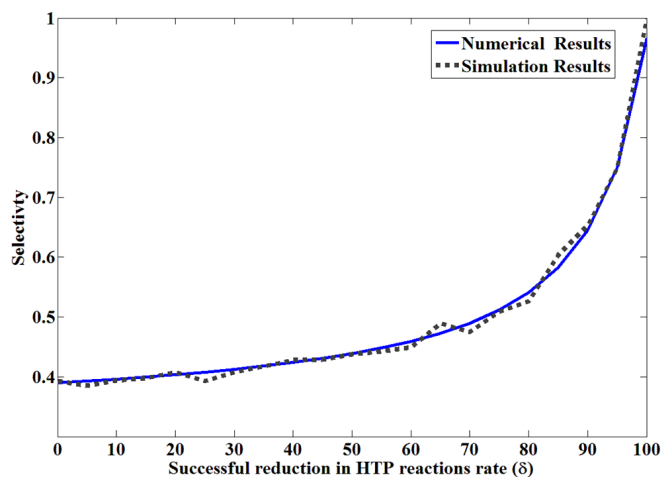


Figure 6.2: Selectivity for different reduction in HTP rate ( $\delta$ ) for CO=5, H=15 based on numerical (solid line) vs. simulation (squares) results.

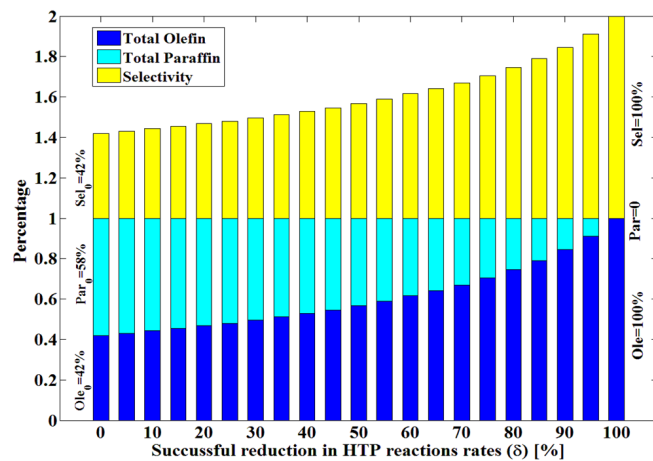


Figure 6.3: Product distribution and selectivity after running the simulation with initial molecules of CO: 10000 and 20000 for different values of  $\delta$ .

of selectivity and product distribution from simulation results. Figure 6.3 shows product distribution and selectivity for 21 different value of  $\delta$  ranging from 0 to 100 in a large scale experiment of CO=10000 and H=20000. It confirms by increasing  $\delta$  (successful reduction in rate of HTP reactions) from 0-100 selectivity increase from 42 to 100, the ratio of olefin ( $C_nH_{2n}$ ) raises from 42 to 100 and finally the ratio of paraffin species ( $C_nH_{2n+2}$ ) drops from 58 to 0.

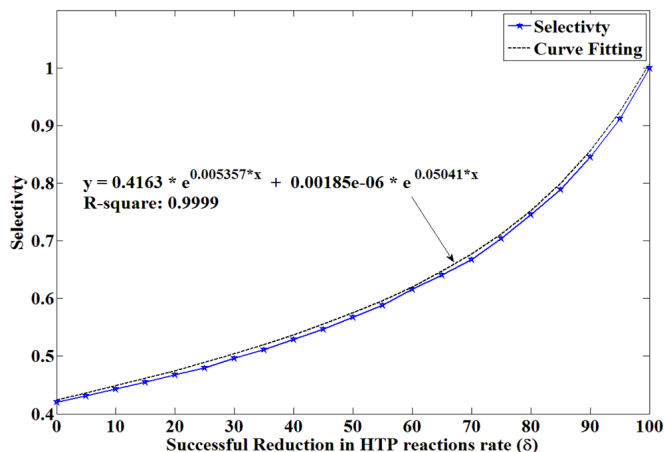


Figure 6.4: Selectivity for different reduction in HTP rate based on large scale simulation (CO=10000, H=20000).

Figure 6.4 reveals an exponential relationship between successful reduction in the rate of HTP reaction ( $\delta$ ) and selectivity. Selectivity starts from 42 in  $\delta=0$  and raise exponentially to 1 in case of  $\delta=100$  which means there is no possibility for HTP reaction. This near real experiment is revealing more selectivity improvement in comparison with its correspondence figure (figure 5.3) in numerical results for small initial reactants. For instance, It shows we can achieve selectivity of 62 which means 53 boosting in selectivity by cutting 60 of HTP reactions ( $\delta=60$ ).

### 6.3 Validating Chemical Properties

The purpose of this part is validating the generated results, specifically product distribution, via acceptable chemical criteria. FT product distribution has initially described with the so called Anderson-Schulz-Flory (ASF) distribution characterized by the chain growth probability factor ( $\alpha$ ) [3]. According to Anderson [36], the product distribution of hydrocarbons can be described by the ASF equation:

$$m_n = (1 - \alpha)\alpha^{(n-1)} \quad (6.1)$$

which  $m_n$  is the mole fraction of a hydrocarbon with chain length  $n$  ( $C_nH_{2n} + C_nH_{2n+2}$ ) and  $\alpha$  is the chain growth probability factor. To calculate chain

growth probability, , we draw the graph of  $\ln(C_nH_{2n} + C_nH_{2n+2})$  for different value of chain length (n) from results of one experiment of  $\delta=0$ . The slope of such curve would be chain growth probability and its equal to 0.6527 for  $\delta=0$ . After calculating chain growth probability then we use equation (2) to draw product distribution based on ASF. To draw product distribution based on simulation results we use the output of SSA to calculate the ratio of each hydrocarbon with degree of n ( $C_nH_{2n} + C_nH_{2n+2}$ ).

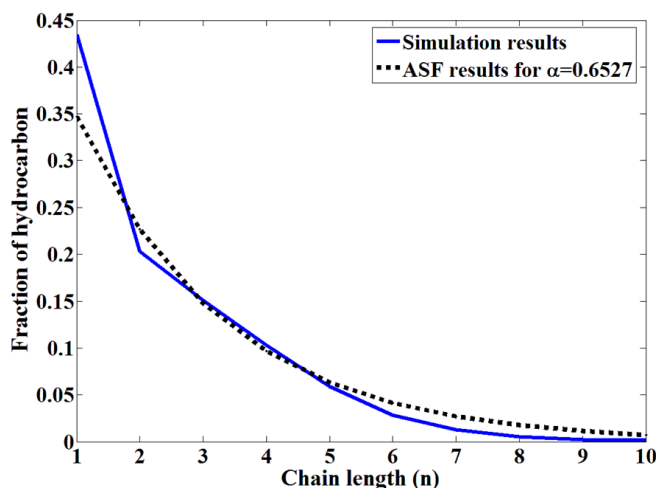


Figure 6.5: Product distribution of a normal FT based on ASF model and simulation results. Both follow same trend and it means our simulation results are valid.

As figure 6.5 reveals, our product distribution for a normal FT synthesis ( $\delta=0$ ) which has been obtained via simulation follows the standard ASF model.

## 7 Discussion

It is clear that success of the proposed NSN in exerting spatial control over H adsorption would depend in turn on its sensing, actuation, and communication capabilities. While NSNs are in their embryonic stages of development, there would be issues with all three dimensions, sensing, actuation, and communication. In [37] we have modeled the effect of the communication reliability on the selectivity assuming perfect sensing and actuation capabilities. But other potential issues from sensing and actuating should be investigated in future works. In a real chemical system, changing in the rate of any reaction will affect other possible reactions if they have common reactants. In FT synthesis, any probable reduction in rate of HTP reactions leads to some side effects via providing more  $C_nH_{2n+1}$  and hydrogen for other reactions which consume  $C_nH_{2n+1}$  or H. As a result, it can lead to at least three main effects: (1) B-dehydrogenation to olefin (DTO) reactions would be more likely to happen as it can find more  $C_nH_{2n+1}$  (2) increasing in the rate of chain growth as it consumes  $C_nH_{2n+1}$  (3) raising in

the rate of water formation reaction as it consume H. In this work, we capture the direct effect of reduction in HTP on the selectivity and product distribution. While some of these effects such as increasing BTO rate has a positive impact on the product selectivity, to capture the real effect of NSN it would be more realistic to involve these side effects as well.

## 8 Conclusion

We have proposed a network of nano-machines, NSN, for monitoring and controlling of the surface of Fischer-Tropsch steps involving hydrogenation to paraffin (HTP) and olefin production at the molecular-level. NSN prevents adsorption of H on sites adjacent to those containing  $C_nH_{2n+1}$  with the ultimate goal of improving olefin selectivity of FT catalysis. We have developed an analytical model based on Markov chain to capture the effect of any reduction in rate of HTP reactions ( $\delta$ ). The numerical results revealed a decrease in the paraffin ( $C_nH_{2n+2}$ ) formation with concomitant increase in olefin production. Indeed, there is an exponential relationship between  $\delta$  and product selectivity. Complementary extensive simulations based on SSA for a large-scale FT synthesis were also in agreement with the MC computational results.

## Bibliography

- [1] Mark E. Dry. Commercial conversion of carbon monoxide to fuels and chemicals. *Journal of Organometallic Chemistry*, 372(1):117–127, August 1989.
- [2] AA Adesina. Hydrocarbon synthesis via Fischer-Tropsch reaction: travails and triumphs. *Applied Catalysis A: General*, 138(2):345–367, May 1996.
- [3] Gerard P. Van Der Laan and a. a. C. M. Beenackers. Kinetics and Selectivity of the FischerTropsch Synthesis: A Literature Review. *Catalysis Reviews*, 41(3-4):255–318, January 1999.
- [4] Wei Chen, Zhongli Fan, Xiulian Pan, and Xinhe Bao. Effect of confinement in carbon nanotubes on the activity of Fischer-Tropsch iron catalyst. *Journal of the American Chemical Society*, 130(29):9414–9, July 2008.
- [5] Nguen Man Tyong, Nguen Chan Khung, I. G. Ivanov, I. V. Baronin, and E. G. Rakov. Fabrication of catalysts for synthesis of carbon nanotubes by wet burning method in continuous apparatus. *Russian Journal of Applied Chemistry*, 82(5):763–766, June 2009.
- [6] Qinghong Zhang, Jincan Kang, and Ye Wang. Development of Novel Catalysts for Fischer-Tropsch Synthesis: Tuning the Product Selectivity. *Chem-CatChem*, 2(9):1030–1058, September 2010.
- [7] NakhaeiPour Ali, Mohammad Reza Housaindokht, Sayyed Faramarz Tayyari, and Jamshid Zarkesh. Deactivation studies of nano-structured iron catalyst in Fischer-Tropsch synthesis. *Journal of Natural Gas Chemistry*, 19(3):333–340, May 2010.

- [8] P. C. Thüne, C. J. Weststrate, P. Moodley, a. M. Saib, J. van de Loosdrecht, J. T. Miller, and J. W. Niemantsverdriet. Studying FischerTropsch catalysts using transmission electron microscopy and model systems of nanoparticles on planar supports. *Catalysis Science & Technology*, 1(5):689, 2011.
- [9] B Todica, T Olewska, N Nikacevicb, and DB Bukur. Modeling of Fischer-Tropsch Product Distribution over Fe-based Catalyst. *CHEMICAL ENGINEERING*, 32(2007):793–798, 2013.
- [10] Ian F. Akyildiz, Fernando Brunetti, and Cristina Blázquez. Nanonetworks: A new communication paradigm. *Computer Networks*, 52(12):2260–2279, August 2008.
- [11] Josep Miquel Jornet, Joan Capdevila Pujol, and Josep Solé Pareta. PHLAME: A Physical Layer Aware MAC protocol for Electromagnetic nanonetworks in the Terahertz Band. *Nano Communication Networks*, 3(1):74–81, March 2012.
- [12] B Atakan and OB Akan. Carbon nanotube-based nanoscale ad hoc networks. *Communications Magazine, IEEE*, 48(6):129–135, 2010.
- [13] Chun Tung Chou. Molecular circuits for decoding frequency coded signals in nano-communication networks. *Nano Communication Networks*, 3(1):46–56, March 2012.
- [14] Chun Tung Chou. Extended Master Equation Models for Molecular Communication Networks. *IEEE Transactions on NanoBioScience*, 12(2):79–92, 2013.
- [15] J. Weldon, K. Jensen, and A. Zettl. Nanomechanical radio transmitter. *Physica Status Solidi (B)*, 245(10):2323–2325, October 2008.
- [16] Julian W. Gardner Bartlett and Philip N. Application of conducting polymer technology in microsystems. *Sensors and Actuators*, 51(1):57–66, 1995.
- [17] EP Giannelis. Polymer layered silicate nanocomposites. *Advanced materials*, 8(1):29–35, 1996.
- [18] Sandeep S. Pendhari, Tarun Kant, and Yogesh M. Desai. Application of polymer composites in civil construction: A general review. *Composite Structures*, 84(2):114–124, July 2008.
- [19] Albert Renken and L Kiwi-Minsker. Microstructured catalytic reactors. *Advances in Catalysis*, 53(10):47–122, 2010.
- [20] P. C. Thüne, C. J. Weststrate, P. Moodley, and a. M. Saib. Studying FischerTropsch catalysts using transmission electron microscopy and model systems of nanoparticles on planar supports. *Catalysis Science & Technology*, 1(5):689, 2011.
- [21] N. Fischer, E. van Steen, and M. Claeys. Preparation of supported nano-sized cobalt oxide and fcc cobalt crystallites. *Catalysis Today*, 171(1):174–179, August 2011.

- [22] Chem Eng and K Dalai. Archive of SID Deactivation Behavior of Carbon Nanotubes Supported Cobalt Catalysts in Fischer-Tropsch Synthesis Archive of SID. 30(1):37–47, 2011.
- [23] Diego a Gómez-Gualdrón, Jin Zhao, and Perla B Balbuena. Nanocatalyst structure as a template to define chirality of nascent single-walled carbon nanotubes. *The Journal of chemical physics*, 134(1):014705, January 2011.
- [24] Heon Ham, No-Hyung Park, Inpil Kang, Hyoun Woo Kim, and Kwang Bo Shim. Catalyst-free fabrication of graphene nanosheets without substrates using multiwalled carbon nanotubes and a spark plasma sintering process. *Chemical communications (Cambridge, England)*, 48(53):6672–4, July 2012.
- [25] J V Lauritsen and F Besenbacher. Model Catalyst Surfaces Investigated by Scanning Tunneling Microscopy. 50:97–147, 2006.
- [26] Rutger a. van Santen, Mohammed Minhaj Ghouri, Sharan Shetty, and Emiel M. H. Hensen. Structure sensitivity of the FischerTropsch reaction; molecular kinetics simulations. *Catalysis Science & Technology*, 1(6):891–911, 2011.
- [27] Ali NakhaeiPour, Mohammad Reza Housaindokht, Sayyed Faramarz Tayyari, and Jamshid Zarkesh. Fischer-Tropsch synthesis by nano-structured iron catalyst. *Journal of Natural Gas Chemistry*, 19(3):284–292, May 2010.
- [28] Joel Villatoro and David Monzón-Hernández. Fast detection of hydrogen with nano fiber tapers coated with ultra thin palladium layers. *Optics express*, 13(13):5087–92, June 2005.
- [29] Chanda Ranjit Yonzon, Douglas a Stuart, Xiaoyu Zhang, and Adam D McFarland. Towards advanced chemical and biological nanosensors-An overview. *Talanta*, 67(3):438–48, September 2005.
- [30] C Falconi, a Damico, and Z Wang. Wireless Joule nanoheaters. *Sensors and Actuators*, 127(1):54–62, October 2007.
- [31] Daniel T. Gillespie. A rigorous derivation of the chemical master equation. *Physica A: Statistical Mechanics and its Applications*, 188(1-3):404–425, September 1992.
- [32] Mor Harchol-balter. *Performance Modeling and Design of Computer Systems*. Cambridge University Press, 2013.
- [33] William J. Stewart. *Probability, Markov Chains, Queues, and Simulation: The Mathematical Basis of Performance Modeling*. Princeton University Press, 2009.
- [34] Antti Valmari. Stubborn sets for reduced state space generation. *Lecture Notes in Computer Science*, 483:491–515, 1991.
- [35] DT Gillespie. Exact stochastic simulation of coupled chemical reactions. *The journal of physical chemistry*, 81(25):2340–2361, 1977.

- [36] R. B. Anderson. Catalysts for the FischerTropsch Synthesis. *Van Nostrand Rein- hold*, 4, 1956.
- [37] Eisa Zarepour, Mahbub Hassan, Chun Tung Chou, and A. A. Adesina. Nano-scale Sensor Networks for Chemical Catalysis. In *The 13th IEEE International Conference on Nanotechnology*, Beijing, China, Aug. 2013.